

## Solid-state NMR studies of the prion protein H1 fragment

JONATHAN HELLER,<sup>1</sup> ANDREW C. KOLBERT,<sup>2,3,6</sup> RUSSELL LARSEN,<sup>2,4,7</sup>  
MATTHIAS ERNST,<sup>2</sup> TATIANA BEKKER,<sup>3</sup> MICHAEL BALDWIN,<sup>3</sup>  
STANLEY B. PRUSINER,<sup>3</sup> ALEXANDER PINES,<sup>2,4</sup> AND DAVID E. WEMMER<sup>2,5</sup>

<sup>1</sup> Graduate Group in Biophysics, University of California, Berkeley, California 94720

<sup>2</sup> Department of Chemistry, University of California, Berkeley, California 94720

<sup>3</sup> Department of Neurology, University of California, San Francisco, California 94143

<sup>4</sup> Materials Sciences Division, Lawrence Berkeley National Laboratory, Berkeley, California 94720

<sup>5</sup> Structural Biology Division, Lawrence Berkeley National Laboratory, Berkeley, California 94720

(RECEIVED February 23, 1996; ACCEPTED April 14, 1996)

### Abstract

Conformational changes in the prion protein (PrP) seem to be responsible for prion diseases. We have used conformation-dependent chemical-shift measurements and rotational-resonance distance measurements to analyze the conformation of solid-state peptides lacking long-range order, corresponding to a region of PrP designated H1. This region is predicted to undergo a transformation of secondary structure in generating the infectious form of the protein. Solid-state NMR spectra of specifically <sup>13</sup>C-enriched samples of H1, residues 109–122 (MKHMAGAAAAGAVV) of Syrian hamster PrP, have been acquired under cross-polarization and magic-angle spinning conditions. Samples lyophilized from 50% acetonitrile/50% water show chemical shifts characteristic of a  $\beta$ -sheet conformation in the region corresponding to residues 112–121, whereas samples lyophilized from hexafluoroisopropanol display shifts indicative of  $\alpha$ -helical secondary structure in the region corresponding to residues 113–117. Complete conversion to the helical conformation was not observed and conversion from  $\alpha$ -helix back to  $\beta$ -sheet, as inferred from the solid-state NMR spectra, occurred when samples were exposed to water. Rotational-resonance experiments were performed on seven doubly <sup>13</sup>C-labeled H1 samples dried from water. Measured distances suggest that the peptide is in an extended, possibly  $\beta$ -strand, conformation. These results are consistent with the experimental observation that PrP can exist in different conformational states and with structural predictions based on biological data and theoretical modeling that suggest that H1 may play a key role in the conformational transition involved in the development of prion diseases.

**Keywords:** chemical shift; prion peptides; rotational resonance; secondary structure; solid-state NMR

Prion diseases arise through a posttranslational change to the prion protein, PrP (Borchelt et al., 1990; Prusiner, 1992). These neurodegenerative illnesses are novel in that they can be transmitted by prions, proteinaceous agents apparently devoid of nucleic acids (Meyer et al., 1991; Kellings et al., 1992), and because they are manifest in sporadic, inherited, and infectious illnesses. The function of the normal cellular protein (PrP<sup>C</sup>), which is expressed ubiquitously on the surface of neurons, is unknown. Gene-targeted mice in which the PrP gene has been disrupted appear to develop and live normally (Büeler et al., 1992),

except that, unlike normal mice, they are resistant to infection by prions (Büeler et al., 1993; Prusiner et al., 1993). In contrast, transgenic mice expressing a mutant PrP transgene encoding a proline to leucine substitution known to cause Gerstmann-Sträussler-Scheinker disease in humans spontaneously develop a transmissible prion disease (Hsiao et al., 1990, 1994).

PrP<sup>C</sup> is a glycosylphosphatidylinositol anchored protein found mostly at the cell surface, from which it can be released by phosphatidylinositol-phospholipase C (Stahl et al., 1987), unlike the pathogenic isoform (PrP<sup>Sc</sup>), which accumulates within the cell (Taraboulos et al., 1990). Many lines of evidence have converged to suggest that the conversion of PrP<sup>C</sup> into PrP<sup>Sc</sup> does not involve a covalent change (Stahl et al., 1993), but is conformational in nature (Pan et al., 1993; Cohen et al., 1994). This posttranslational event gives rise to different physical properties (Borchelt et al., 1990). PrP<sup>C</sup> is soluble in nonionic detergents and is protease sensitive. PrP<sup>Sc</sup> is insoluble and proteolysis

Reprint requests to: David E. Wemmer, Department of Chemistry, University of California, Berkeley, California 94720-1460; e-mail: dewemmer@lbl.gov.

<sup>6</sup> Present address: DSM Copolymer, P.O. Box 2591, Baton Rouge, Louisiana 70821.

<sup>7</sup> Present address: Department of Chemistry, University of Iowa, Iowa City, Iowa 52242.

cleaves only the N-terminal third of the sequence, leaving a protease-resistant core termed PrP 27–30, which retains infectivity; in the presence of Sarkosyl, this rearranges into amyloid rods that stain with Congo red and show green-gold birefringence (Prusiner et al., 1983; McKinley et al., 1991). Fourier transform infrared spectroscopy (FTIR) and CD have demonstrated that PrP<sup>C</sup> is rich in  $\alpha$ -helices and virtually devoid of  $\beta$ -sheet (Pan et al., 1993), unlike PrP<sup>Sc</sup> and PrP 27–30, which have a high  $\beta$ -sheet content (Caughey et al., 1991; Pan et al., 1993; Safar et al., 1994).

Secondary structure analysis based on sequence homology and molecular modeling predicted that PrP<sup>C</sup> contains four  $\alpha$ -helices, designated H1–H4. Biological data suggest that it is the first two of these helices that convert to  $\beta$ -sheet in PrP<sup>Sc</sup> (Huang et al., 1994, 1996). When peptides corresponding to these four regions were synthesized, three of them were found to have very low solubility in H<sub>2</sub>O, and FTIR, CD, and electron microscopy showed that they formed  $\beta$ -sheets and polymerized into fibrils (Gasset et al., 1992; Nguyen et al., 1995a). However, CD and solution NMR studies in organic solvents, such as hexafluoroisopropanol (HFIP), or detergents, such as SDS, have shown that H1 and H2, as well as peptides corresponding to longer segments of PrP containing these regions, can form  $\alpha$ -helices (Zhang et al., 1995). Thus, these synthetic peptides seem to be able to model some aspects of the conformational pluralism that are exhibited by PrP.

To date, both the cellular and scrapie isoforms of PrP have proven intractable to high-resolution spectroscopic or crystallographic study. PrP<sup>Sc</sup> is particularly problematic because it is insoluble and forms aggregates lacking long-range order (Nguyen et al., 1995b). Solid-state NMR is one of the few techniques able to answer specific structural questions about peptides or proteins in immobile states, such as aggregated peptides and membrane proteins, through the use of chemical-shift information and specific distance measurements. We have used solid-state NMR to gain structural information about an aggregated form of the first of the predicted structural regions, H1 (residues 109–122 of the Syrian hamster PrP sequence).

It has been shown that <sup>13</sup>C chemical shifts are highly correlated with peptide secondary structure in the solid state (Kricheldorf & Muller, 1983; Saito, 1986). We have employed cross-polarization/magic-angle spinning (CPMAS) techniques (Pines et al., 1973; Schaefer & Stejskal, 1976) to determine chemical shifts of specifically <sup>13</sup>C-labeled H1 peptides, and used this information to gain insight into the overall secondary structure of these peptides. <sup>13</sup>C CPMAS spectra can yield isotropic chemical shifts with relatively high accuracy. These chemical shifts predominately reflect the local conformations of the peptides and are largely independent of the identity of neighboring residues. Conformations of  $\alpha_R$ -helix,  $\alpha_L$ -helix,  $\omega$ -helix,  $3_{10}$  helix, and  $\beta$ -sheet can be distinguished on the basis of chemical shift. Chemical shifts of amino acid carbons in the solid state in a  $\beta$ -sheet conformation differ by as much as 8 ppm from those in an  $\alpha$ -helix (Saito, 1986). Similarly strong correlations have been seen in solution (Spera & Bax, 1991; Wishart & Sykes, 1994), and reproduced in recent theoretical work (de Dios et al., 1993). By using CPMAS to determine isotropic shifts, meaningful information about secondary structure of aggregated proteins can be gained.

We have also used internuclear distance-measurement techniques with doubly <sup>13</sup>C-labeled peptides to determine specific

distances. Types of secondary structure can be distinguished and structural details discovered best through the measurement of a large number of distances. Strong homonuclear dipolar couplings in solids prevent the use of solution-state proton NMR experiments, such as NOESY (Jeener et al., 1979) and TOCSY (Braunschweiler & Ernst, 1983; Davis & Bax, 1985). Thus, alternative techniques must be employed to determine distances in solids, and recently many such techniques have been designed (Raleigh et al., 1988; Gullion & Schaefer, 1989; Tycko & Dabaghi, 1990; Ishii & Terao, 1995). Rotational-resonance ( $R^2$ ) magnetization exchange (Raleigh et al., 1988; Levitt et al., 1990) is a homonuclear distance-measurement technique that has been applied to several biological systems (Creuzet et al., 1991; Smith et al., 1994b), including one amyloid system (Lansbury et al., 1995). For carbon labels, the technique can be used to measure distances of about 7 Å, with no  $R^2$  effects indicating that the distance between a pair of <sup>13</sup>C labels is greater than about 7 Å.

## Results and discussion

### Chemical shifts

The isotropic shifts of carbonyl <sup>13</sup>C labels throughout the H1 fragment were measured after lyophilization both from acetonitrile (AcN)/H<sub>2</sub>O and from HFIP. Chemical-shift changes on the order of 3 ppm were observed for <sup>13</sup>C resonances when the solvent was changed, although samples lyophilized from HFIP showed an additional minor component retaining the chemical shift of the form lyophilized from AcN/H<sub>2</sub>O. Figure 1 shows the CPMAS spectra for a sample of a mixture of alanine 115 <sup>13</sup>C=O, <sup>13</sup>C $\alpha$ , and <sup>13</sup>CH<sub>3</sub>-labeled H1 peptides lyophilized from AcN/H<sub>2</sub>O (Fig. 1A) and from HFIP (Fig. 1B). Because con-

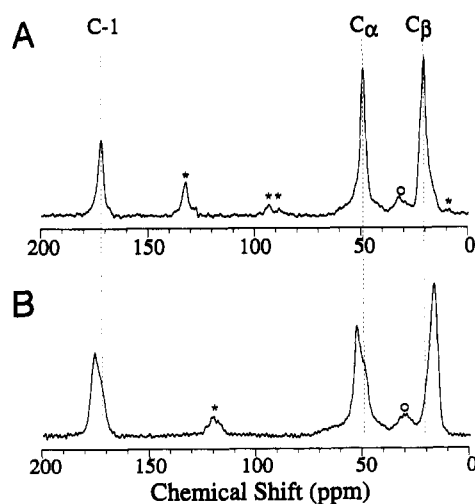


**Fig. 1.** **A:** CPMAS spectrum of a mixture of alanine 115 <sup>13</sup>C=O, <sup>13</sup>C $\alpha$ , and <sup>13</sup>CH<sub>3</sub> labeled H1 peptides lyophilized from 50% AcN/50% H<sub>2</sub>O. Sixty-four scans were acquired with a CP contact time of 2.0 ms, and a recycle delay of 1.5 s. Spinning speed was approximately 3.0 kHz. Peaks marked with "\*" are spinning sidebands; those marked with "o" are due to natural-abundance background <sup>13</sup>C. All chemical shifts are referenced to <sup>13</sup>C=O glycine at 176.04 ppm. **B:** CPMAS spectrum of the same peptides lyophilized from HFIP. The same experimental parameters as in A were used. Dotted lines indicate the positions of the lines when lyophilized from 50% AcN/50% H<sub>2</sub>O.

version of the sample to the HFIP form was only approximately 70%, and the two peaks were not completely resolved, we fit each HFIP spectral line with two Lorentzians to obtain accurate chemical shifts. Our data indicate that H1 can exist in at least two different conformations in the solid state, depending on the solvent from which the sample is lyophilized. We define the secondary structure index,  $\chi_{SS}$ , in a similar way to Wishart and Sykes (1994), as a measure of the degree to which a  $^{13}\text{C}$ 's chemical shift agrees with literature values for either  $\alpha$ -helix or  $\beta$ -sheet:

$$\chi_{SS} = 2 * \frac{\delta_{\text{expt}} - \bar{\delta}_{\text{lit}}}{\Delta\delta_{\text{lit}}},$$

where  $\delta_{\text{expt}}$  is the experimentally determined chemical shift,  $\bar{\delta}_{\text{lit}}$  is the average of the literature values of the chemical shifts for a particular residue in an  $\alpha$ -helix and in a  $\beta$ -sheet (Saito, 1986) (when more than one literature value for a residue in a particular conformation exists, an average of these values is taken before the  $\bar{\delta}_{\text{lit}}$  is calculated), and  $\Delta\delta_{\text{lit}} = \bar{\delta}_{\beta} - \bar{\delta}_{\alpha}$  is the difference of shifts for a particular residue in an  $\alpha$ -helix and in  $\beta$ -sheet.  $\chi_{SS}$  is +1 when the chemical shift is in perfect agreement with literature values for a sheet conformation, whereas it is -1 when it is in perfect agreement with published values for the  $\alpha$ -helix conformation. Trends in the secondary structure index are indicative of types of secondary structure, even in the presence of some outliers. When lyophilized from AcN/H<sub>2</sub>O, carbonyl (Fig. 2), C <sub>$\alpha$</sub>  and C <sub>$\beta$</sub>  chemical shifts throughout the peptide agree reasonably well with literature values for  $\beta$ -sheet. Glycine 119 carbonyl shows two resolved resonances, indicating that more than one conformation is present in our polycrystalline sample. The chemical shift of one of these resonances is consistent with the  $\beta$ -sheet conformation, whereas the other is likely to be some sort of turn, because its chemical shift is similar to the chemical shifts for helical forms. Carbonyl secondary structure indices for the AcN/H<sub>2</sub>O form, from residue 112 to 122 are: 0.5, 0.4, 1.2, 0.7, 0.8, 0.6, 0.5, 0.9 (-1.8), 0.6, 0.1, -1.4. The chemical shifts of the major component of samples prepared from HFIP show secondary structure indices indicative of  $\alpha$ -helical conformation. Indices of the minor components remain indicative of  $\beta$ -sheet, although low signal-to-noise and errors in fitting make the precision of these calculations lower. The indices for the HFIP form's major (minor) peak for the carbonyl carbons of residues 112 to 120 are: -0.4 (0.7), -0.9 (0.1), -1.3, -0.7 (0.7), -0.9 (0.4), -1.0 (0.1), -0.3 (0.4), -2.2 (0.3), -0.1 (0.4). No minor peak was observed for glycine 114.

Samples lyophilized from HFIP were found to be water sensitive. Chemical shifts for these samples were observed to change after exposure to water vapor. Figure 3A is the spectrum of the mixture of alanine 115-labeled peptides lyophilized from HFIP. The shifts of the three lines are in good agreement with the helical conformation, with  $\chi_{SS} = -0.7$ , -1.0, and -0.7 for the  $^{13}\text{C}=\text{O}$ ,  $^{13}\text{C}_{\alpha}$ , and  $^{13}\text{CH}_3$  lines, respectively. When the samples were exposed to an environment of 30% humidity (H<sub>2</sub>O vapor over a saturated solution of CaSO<sub>4</sub> at 25 °C), for 30 min, partial conversion back to the other conformation was observed, as illustrated in Figure 3B. Figure 3C illustrates the spectrum after exposing the sample to 100% humidity for 2 h. The lines then occur at a chemical shift indicative of a pure  $\beta$ -sheet conformation, with  $\chi_{SS} = 0.7$ , 0.6, and 1.36 for the  $^{13}\text{C}=\text{O}$ ,  $^{13}\text{C}_{\alpha}$ , and  $^{13}\text{CH}_3$  lines, respectively. We interpret this to mean that the he-

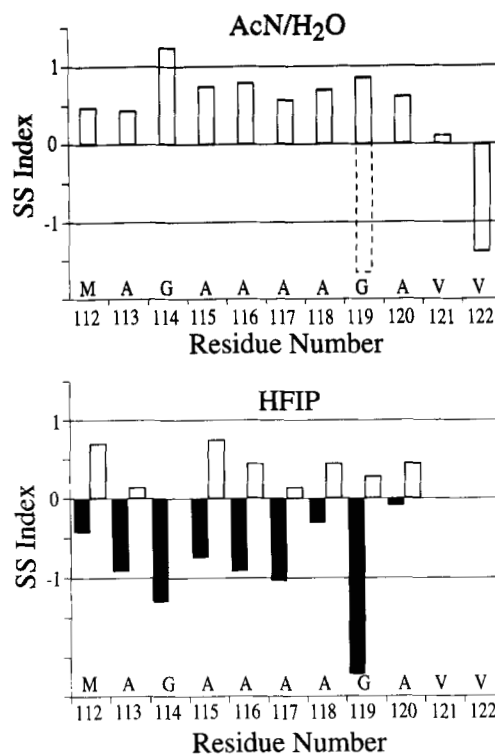


**Fig. 2.** Carbonyl secondary structure index values for the central residues of the H1 peptide obtained from CPMAS spectra of singly-labeled peptides. A value of +1 (-1) indicates perfect agreement with published chemical shifts of that residue type in a  $\beta$ -sheet ( $\alpha$ -helix) conformation. Chemical shifts for the HFIP form were obtained by line-fitting spectra; filled bars indicate the secondary structure index value for the main peak (>70%); white bars indicate the secondary structure index value for the minor peak. Published carbonyl chemical-shift data in ppm are as follows (Saito, 1986): alanine ( $\beta$ -sheet): 171.8, 171.6, and 172.2; alanine ( $\alpha$ -helix): 176.4, 176.2, and 176.8; glycine ( $\beta$ -sheet): 168.5, 168.4, and 168.5; glycine ( $\alpha$ -helix): 171.7, 171.4, 172.0, and 172.1; methionine ( $\beta$ -sheet): 170.6; methionine ( $\alpha$ -helix): 175.1; valine ( $\beta$ -sheet): 171.5 and 171.8; valine ( $\alpha$ -helix): 174.9. Larger errors are expected in the HFIP data due to the need to fit two unresolved peaks to acquire chemical shifts.

lical form obtained from HFIP is only meta-stable in the solid state, and when water is present, a sheet form is preferred.

#### Rotational resonance

A total of seven C=O—C <sub>$\alpha$</sub>  distances were measured in H1 (Table 1) and compared with distances expected from idealized  $\alpha$ -helix and  $\beta$ -sheet conformations. From these idealized models and the experimental and fitting precision, it appears that, although rotational resonance can be used to measure  $i$  to  $i + 1$  and  $i$  to  $i + 2$  distances, the precision is insufficient to distinguish between types of secondary structure. Thus,  $i$  to  $i + 3$  distances are better indicators of types of secondary structure.

An issue that becomes important in our measurements is sample inhomogeneity (Heller et al., 1996). Because the samples showed significant inhomogeneous broadening (as determined by spin-echo experiments) and the rotational-resonance condition is fairly narrow, the rotational-resonance condition may not be satisfied simultaneously by all isochromats of the lines. Thus,

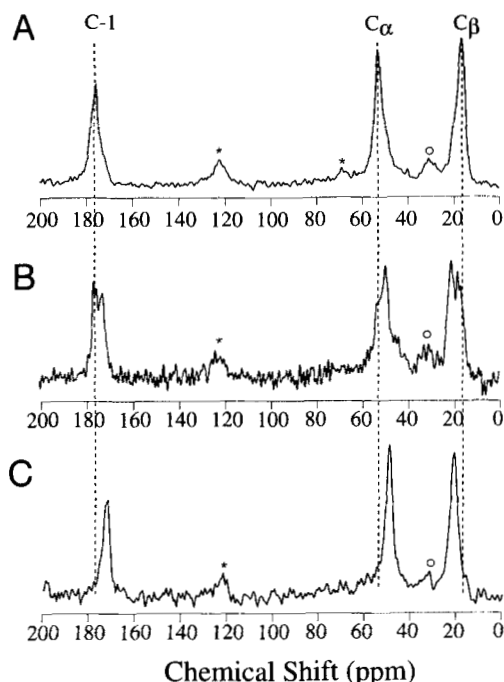


**Fig. 3.** CPMAS spectra of a mixture of alanine 115  $^{13}\text{C}=\text{O}$ ,  $^{13}\text{C}_\alpha$ , and  $^{13}\text{CH}_3$  H1 peptides (A) lyophilized from HFIP; (B) after exposure to air at 30% humidity ( $\text{H}_2\text{O}$  vapor over a saturated solution of  $\text{CaSO}_4$  at  $25^\circ\text{C}$ ) for 30 min; (C) after 2-h exposure to air at 100% humidity. Experimental parameters are as in Figure 1, except the number of scans was 1,024 for A, 2,384 for B, and 512 for C, and less sample was used. Peaks marked with "\*" are spinning sidebands and those marked with "o" are due to natural-abundance background  $^{13}\text{C}$ . Dotted lines indicate the positions of the shifts when lyophilized from HFIP.

they cannot undergo efficient magnetization exchange, and the measured distances appear systematically longer than the "true" distance. We account for such off rotational-resonance effects due to incomplete correlation between inhomogeneous lines in our simulations (Heller et al., 1996), and thus obtain accurate distances.

For short distances, we fit the distance, the  $T_{2ZQ}$ , and the inhomogeneous line width simultaneously. Because, in the case of short distances, the three parameters are not highly correlated

**Table 1.** Measured and theoretical distances for the seven doubly-labeled H1 peptides

C=O label	$\text{C}_\alpha$ label	Best fit distance (Å)	Minimum distance (Å)	Maximum distance (Å)	$\alpha$ -Helical distance <sup>a</sup> (Å)	$\beta$ -Sheet distance <sup>a</sup> (Å)
115	116	2.4	2.3	2.5	2.4	2.4
115	117	5.8	5.4	7.8	4.5	5.4
115	118	5.8	5.6	7.8	4.5	8.8
114	115	2.4	2.3	2.5	2.4	2.4
113	115	5.4	4.9	7.2	4.5	5.4
114	117	6.6	6.3	8.5	4.5	8.8
113	116	6.0	5.6	7.7	4.5	8.8

<sup>a</sup> Distances derived from idealized  $\alpha$ -helical and  $\beta$ -strand conformations.

(cross-correlation coefficients of  $\rho < 0.6$ ), the distance,  $T_{2ZQ}$ , and inhomogeneous line width can simultaneously be obtained for these samples. We assume these parameters are transferable between samples. Figure 4A shows the data and fit for a measurement of the distance from glycine 114 C=O to alanine 115  $\text{C}_\alpha$ . The best fit gave a distance of 2.37 Å, which is within experimental error of the correct distance of approximately 2.42 Å. The value of the zero-quantum relaxation time, 9.5 ms, was longer than expected from the  $T_2$  values (Kubo & McDowell, 1988) of the individual lines ( $5.0 \pm 0.4$  ms for the carbonyl and  $6.7 \pm 0.7$  ms for the  $\text{C}_\alpha$ ). The inhomogeneous line width obtained, 76.3 Hz (full width at half height), indicates some correlation between the C=O and  $\text{C}_\alpha$  peak, but not complete correlation. This agrees well with the results of experiments designed to measure this correlation (Heller et al., 1996). In the case of longer distances, the three parameters are highly correlated (cross-

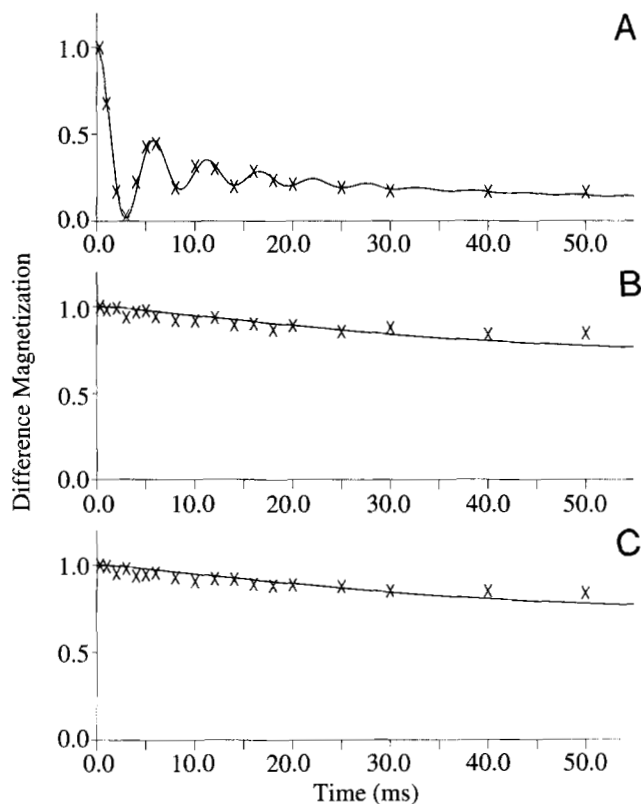


**Fig. 4.** Experimental rotational-resonance magnetization-exchange curves and best fits for doubly  $^{13}\text{C}$ -labeled H1 peptides. A: For a peptide labeled at the C=O of glycine 114 and the  $\text{C}_\alpha$  of alanine 115, values of the three-parameters fit were: distance = 2.37 Å;  $T_{2ZQ}$  = 9.5 ms; inhomogeneous line width  $\Delta\nu_{1/2}$  = 152.6 Hz (full width at half height). Correlation coefficients were all less than 0.6. Thirty-two scans for each of the 18 experimental time points were collected 16 times. B: For a peptide labeled at C=O of alanine 115 and the  $\text{C}_\alpha$  of alanine 117, values of the  $T_{2ZQ}$  and the inhomogeneous line width were fixed at values obtained in A, and the distance was fit to 5.78 Å. Sixty-four scans for each of the 18 experimental time points were collected 11 times. C: For a peptide labeled at C=O of alanine 115 and the  $\text{C}_\alpha$  of alanine 118, values of the  $T_{2ZQ}$  and the inhomogeneous line width were fixed at values obtained in A, and the distance was fit to 5.81 Å. Sixty-four scans for each of the 18 experimental time points were collected seven times. Error bars indicating experimental precision (not shown) are smaller than the symbols.

correlation coefficients of  $\rho \sim 0.9$ ). Thus, the results of a simultaneous fit to all three parameters are not meaningful. The values of the  $T_{2ZQ}$  and the inhomogeneity obtained in the fits of  $i$  to  $i + 1$  peptides were therefore used as fixed constants for fits of the distance for the other peptides. Figures 4B and C show the data and simulations for peptides labeled at the C=O of alanine 115 and the C $_{\alpha}$  of alanine 117, and the same carbonyl and the C $_{\alpha}$  of alanine 118. Distances measured and estimated errors are listed in Table 1.

The rotational-resonance data are consistent with an extended conformation for H1. Distances expected for a  $\beta$ -sheet conformation are slightly longer than the three  $i$  to  $i + 3$  distance measured, but could be consistent with a bent  $\beta$ -sheet model. More distance measurements and greater accuracy would allow the solution of the structure of the H1 peptide to higher resolution.

## Conclusions

From our distance measurements and chemical-shift data, it appears that H1 forms an extended, primarily  $\beta$ -sheet-like conformation when lyophilized from AcN/H<sub>2</sub>O or dried from pure H<sub>2</sub>O. When lyophilized from HFIP, incomplete conversion to the second conformation and overlapping residues make distance measurement more difficult. However, the chemical-shift data from the HFIP form are consistent with the presence of an  $\alpha$ -helix. This  $\alpha$ -helical conformation appears to be only metastable, and reverts to an extended conformation when exposed to water vapor. The observed conversion is consistent with earlier FTIR data for the peptides (Gasset et al., 1992). Additionally, the present study defines the specific residues involved in secondary structure, and, interestingly, shows that the same sequence of residues is involved in the  $\alpha$ -helical or  $\beta$ -sheet conformation. Structural predictions for the protein from molecular modeling (Huang et al., 1994, 1996), and the hypothesis that the infectivity of PrP is the result of a conformational change in H1 and surrounding regions of the protein (Cohen et al., 1994), are also consistent with the present study. Clearly, caution is required when comparing results from this isolated peptide to the corresponding region of the entire PrP molecule.

It may also be of interest to note that our results are similar to those of a solid-state NMR study of a portion of the A $\beta$  peptide found in amyloid deposits in the brains of patients of Alzheimer's disease. Data on the A $\beta$  peptide residues 34–42 suggested a  $\beta$ -sheet or bent  $\beta$ -sheet conformation around a Gly-Gly bond (Lansbury et al., 1995).

The physical properties of the  $\beta$ -sheet-rich PrP<sup>Sc</sup> make it unlikely that high-resolution structural data will be obtained by conventional crystallographic or solution NMR approaches. Thus, there is considerable promise for a method such as solid-state NMR, capable of defining the local environment of individual atoms in a solid lacking long-range order and measuring interatomic distances. At present, the major disadvantage of this approach to defining the structure of a complex entity such as large peptide or protein is the substantial number of specifically labeled peptides required. Despite this limitation, further studies of longer PrP peptides incorporating multiple putative sites of secondary structure, such as peptide 90–145, containing both H1 and H2 (Zhang et al., 1995), are in progress. Eventually, it should be possible to extend these investigations to the entire PrP<sup>Sc</sup> molecule.

## Materials and methods

### Sample preparation

The labeled PrP peptides, with amidated C-termini, were synthesized using N-Fmoc protected amino acids on a Millipore (Bedford, Massachusetts) model 9050 Plus PepSynthesizer. <sup>13</sup>C-labeled Fmoc-amino acids were purchased either from Cambridge Isotope Laboratories (Woburn, Massachusetts), or Isotec (Miamisburg, Ohio). Peptides were purified by reverse-phase HPLC and then lyophilized, dissolved in dilute HCl, and re-lyophilized to remove residual TFA. The purity and incorporation of <sup>13</sup>C labels was confirmed by mass spectrometry. For CPMAS chemical-shift measurements, singly <sup>13</sup>C-labeled samples were then redissolved in 50% AcN/50% H<sub>2</sub>O or 100% HFIP and lyophilized into a powder.

In order to obtain narrower NMR spectral lines for rotational-resonance experiments, doubly <sup>13</sup>C-labeled samples were dissolved in excess H<sub>2</sub>O, partially dried by blowing air over them, and then allowed to equilibrate in an atmosphere of 78% humidity over a saturated solution of ammonium chloride at 25 °C. Line widths obtained from this method were narrower than those from lyophilized samples, reflecting a structurally more homogenous sample. Intermolecular effects in distance measurements were minimized by diluting labeled samples approximately 1:9 in unlabeled H1, except for the two samples with short (i.e.,  $r_{cc} \leq 2.5$  Å) distances in which intermolecular contributions were negligible.

### Data acquisition

All experiments were performed on a home-built spectrometer operating at a <sup>1</sup>H Larmor frequency of 301.2 MHz. For the CPMAS experiments used to measure chemical shifts, a home-built double-resonance probe was used. The <sup>1</sup>H decoupling field strength was 62 kHz, the CP contact time was 2 ms, and the recycle delay was set to 2 s. A Chemagnetics (Fort Collins, Colorado) 4-mm double-resonance high-speed spinning probe was used for rotational-resonance experiments. Spinning speeds were controlled using a home-built spinning-speed controller using a phase-locked loop as the central element in the control circuit. Spinning speeds could be controlled to within  $\pm 10$  Hz with long-term stability. CP contact time was 2.5 ms and the <sup>1</sup>H decoupling field strength was 100 kHz.

For rotational-resonance magnetization-exchange experiments, total experiment times were kept constant by introducing a variable delay while <sup>13</sup>C magnetization was stored along the  $z$ -axis before inversion (Tomita et al., 1994). This led to the same average power dissipation due to proton decoupling in all experiments, thus eliminating radio-frequency heating effects as a possible source of error in the measurements. By observing natural-abundance peaks throughout the experiment, it was confirmed that all changes in signal intensity were due to magnetization exchange. Two hundred fifty-six scans were acquired and discarded at the start of each series of experiments to allow for spectrometer and probe stabilization. The  $n = 1$  rotational-resonance condition was used for all experiments (Levitt et al., 1990). Recycle delays were 5.0 s. Weak pulses or DANTE sequences (Morris & Freeman, 1978) were used to invert the carbonyl resonance. To account for spectrometer drift and to determine experimental precision, the following protocol was

utilized. For each slice, 32 or 64 scans were collected and 18 magnetization exchange time points were sampled in random order (Peerson et al., 1995). This 18-time point experiment was cycled through repeatedly, and experiments for each time point were averaged and analyzed statistically to determine mean values and standard deviations of the experimental data. Natural-abundance contributions to the two lines were calculated by comparing natural-abundance peaks in the methyl region of the spectra with the same peaks in the spectrum of unlabeled H1, and using this scaling factor to calculate the amount of natural-abundance  $^{13}\text{C}$  under the labeled peaks (Peerson et al., 1995). Because these contributions do not undergo magnetization exchange, they were subtracted out before the difference magnetization was calculated. This difference magnetization as a function of rotational-resonance time was used in the  $R^2$  fitting procedure described below.

#### Line fitting

In CPMAS experiments to determine chemical shifts, samples lyophilized from HFIP gave spectra with two partially resolved resonances. One of these lines appeared at the chemical shift of the AcN/H<sub>2</sub>O form, and was interpreted to be due to incomplete conversion to the HFIP form. For these spectra, chemical shifts and line widths were obtained by fitting lines using two Lorentzians with FELIX (Biosym, La Jolla, California). The fit values of chemical shifts were then used in data analysis.

#### Rotational-resonance simulations

Rotational-resonance magnetization-exchange simulations, including corrections for inhomogeneous broadening, and  $\chi^2$  minimizations using model data generated using Floquet theory (Shirley, 1965; Vega, 1992; Levante et al., 1995), were written using the simulation environment GAMMA (Smith et al., 1994a) and are discussed elsewhere (Heller et al., 1996). Three-parameter fits were performed on samples of known, short distances ( $i_{C=O}$  to  $i + I_{C\alpha}$ ) to obtain values for the zero-quantum relaxation times ( $T_{2ZQ}$ ) and for the correlation between inhomogeneous line widths. Using these values, one-parameter minimizations were performed to obtain distances for all other samples. The values for the chemical-shift anisotropies and orientations were held fixed for all simulations. The assumed assignment of the relative orientation of the chemical-shift principal axes should introduce only a small additional error in the distance measurements because the  $n = 1$  rotational-resonance condition is not very sensitive to these parameters (Raleigh et al., 1989; Thompson et al., 1992).

The errors of the optimized distances were calculated as follows. For shorter distances, errors were taken to be two standard deviations as determined by the three-parameter fit. For longer distances, in order to obtain a lower bound for the distance consistent with an experimental data set, a one-parameter fit of the distance was run, setting  $T_{2ZQ}$  equal to the shortest estimated value and using the largest possible degree of inhomogeneous broadening. The upper bound for the distance came from a one-parameter fit of the distance, using the longest possible  $T_{2ZQ}$  value and the smallest possible amount of inhomogeneous broadening. The maximum  $T_{2ZQ}$  was taken to be 1.5 times the fit  $T_{2ZQ}$ , whereas its minimum was calculated using the method of Kubo and McDowell (1988), i.e.,

$$\frac{1}{T_{2ZQ}} = \frac{1}{T_2^{(a)}} + \frac{1}{T_2^{(b)}}$$

where  $a$  and  $b$  are the two spins involved, and the  $T_2$  values were obtained from rotor-synchronized CPMG experiments taken with the MAS frequency away from the rotational-resonance condition. The maximum inhomogeneity was taken to be the line width of the broader of the two peaks, and its minimum was taken to be 0 Hz.

#### Acknowledgments

The work in Berkeley was funded by the Director, Office of Energy Research, Office of Basic Energy Sciences, Materials Sciences Division, U.S. Department of Energy, under contract no. DE-AC03-76SF0098. The research at UCSF was supported by NIH (NS14069, AG08967, AG02132, NS22786), the American Health Assistance Foundation, the Sherman Fairchild Foundation, and the Bernard Osher Foundation. J.H. gratefully acknowledges the Howard Hughes Medical Institute for a predoctoral fellowship. M.E. thanks the Deutsche Forschungsgemeinschaft for the postdoctoral fellowship (grant Er214/1-1). We also thank Steve Smith, Yale University, and Ann McDermott, Columbia University, for providing us with preprints and Malcolm Levitt, Universiteit Stockholm, for helpful discussions.

#### References

- Borchelt DR, Scott M, Taraboulos A, Stahl N, Prusiner SB. 1990. Scrapie and cellular prion proteins differ in their kinetics of synthesis and topology in cultured cells. *J Cell Biol* 110:743-752.
- Braunschweiler BL, Ernst RR. 1983. Coherence transfer by isotropic mixing: Application to proton correlation spectroscopy. *J Magn Reson* 53: 521-528.
- Büeler H, Aguzzi A, Sailer A, Greiner RA, Auenried P, Aguet M, Weissmann C. 1993. Mice devoid of PrP are resistant to scrapie. *Cell* 73:1339-1347.
- Büeler H, Fisher M, Lang Y, Bluethmann H, Lipp HP, DeArmond SJ, Prusiner SB, Aguet M, Weissmann C. 1992. Normal development and behaviour of mice lacking the neuronal cell-surface PrP protein. *Nature* 356:577-582.
- Caughey BW, Dong A, Bhat KS, Ernst D, Hayes SF, Caughey WS. 1991. Secondary structure analysis of the scrapie-associated protein PrP27-30 in water by infrared spectroscopy. *Biochemistry* 30:7672-7680.
- Cohen FE, Pan KM, Huang Z, Baldwin M, Fletterick RJ, Prusiner SB. 1994. Structural clues to prion replication. *Science* 264:530-531.
- Creuzet F, McDermott A, Gebhard R, van der Hoef K, Spijker-Assink B, Herzfeld J, Lugtenburg J, Levitt MH, Griffin RG. 1991. Determination of membrane protein structure by rotational resonance NMR: Bacteriorhodopsin. *Science* 251:783-786.
- Davis DG, Bax A. 1985. Assignment of complex  $^1\text{H}$  NMR spectra via two-dimensional homonuclear Hartmann-Hahn spectroscopy. *J Am Chem Soc* 107:2820.
- de Dios AC, Pearson JG, Oldfield E. 1993. Secondary and tertiary structural effects on protein NMR chemical shifts: An ab initio approach. *Science* 260:1491-1496.
- Gasset M, Baldwin MA, Lloyd D, Gabriel JM, Holtzman DM, Cohen F, Gletterick R, Prusiner SB. 1992. Predicted  $\alpha$ -helical regions of the prion protein when synthesized as peptides form amyloid. *Proc Natl Acad Sci USA* 89:10940-10944.
- Gullion T, Schaefer J. 1989. Rotational-echo double-resonance NMR. *J Magn Reson* 81:196-200.
- Heller J, Larsen R, Ernst M, Kolbert A, Baldwin M, Prusiner SB, Wemmer DE, Pines A. 1996. Application of rotational resonance to inhomogeneously broadened systems. *Chem Phys Lett* 251:223-229.
- Hsiao KK, Groth D, Scott M, Yang SL, Serban H, Rapp D, Foster D, Torchia M, DeArmond SJ, Prusiner SB. 1994. Serial transmission in rodents of neurodegeneration from transgenic mice expressing mutant prion protein. *Proc Natl Acad Sci USA* 91:9126-9130.
- Hsiao KK, Scott M, Foster D, Groth DF, DeArmond SJ, Prusiner SB. 1990. Spontaneous neurodegeneration in transgenic mice with mutant prion protein. *Science* 250:1587-1590.
- Huang Z, Gabriel JM, Baldwin MA, Fletterick RJ, Prusiner SB, Cohen FE.

1994. Proposed three dimensional structure for the cellular prion protein. *Proc Natl Acad Sci USA* 91:7139-7143.
- Huang Z, Prusiner SB, Cohen FE. 1996. Scrapie prions: A three-dimensional model of an infectious fragment. *Folding & Design* 1:13-19.
- Ishii Y, Terao T. 1995. Determination of interheteronuclear distances by observation of the Pake-doublet patterns using the MLEV-8 sequences with composite pulses. *J Magn Reson A* 115:116-118.
- Jeener J, Meier BH, Bachman P, Ernst RR. 1979. Investigation of exchange processes by two-dimensional NMR spectroscopy. *J Chem Phys* 71:4546-4553.
- Kellings K, Meyer N, Miranda C, Prusiner SB, Riesner D. 1992. Further analysis of nucleic acids in purified scrapie prion preparations by improved return refocussing gel electrophoresis (RRGE). *J Gen Virol* 73:1025-1029.
- Kricheldorf HR, Muller D. 1983. Secondary structure of peptides. 3.  $^{13}\text{C}$  NMR cross polarization/magic angle spinning spectroscopic characterization of solid polypeptides. *Macromolecules* 16:615-623.
- Kubo A, McDowell CA. 1988. Spectral spin diffusion in polycrystalline solids under magic-angle spinning. *J Chem Soc Faraday Trans 1* 84:3713-3730.
- Lansbury PTJ, Costa PR, Griffiths JM, Simon EJ, Auger M, Halverson KJ, Kocisko DA, Hendsch ZS, Ashburn TT, Spencer RGS, Tidor B, Griffin RG. 1995. Structural model for the  $\beta$  amyloid fibril: Interstrand alignment of an antiparallel  $\beta$  sheet comprising a C-terminal peptide. *Nature Structural Biol* 2:990-998.
- Levante TO, Baldus M, Meier BH, Ernst RR. 1995. Formalized quantum mechanical Floquet theory and its application to sample spinning in nuclear magnetic resonance. *Mol Phys* 86:1195-1212.
- Levitt MH, Raleigh DP, Cruzet R, Griffin RG. 1990. Theory and simulations of homonuclear spin pair systems in rotating solids. *J Chem Phys* 92:6347-6364.
- McKinley MP, Meyer RK, Kenaga L, Rahbar F, Cotter R, Serban A, Prusiner SB. 1991. Scrapie prion rod formation in vitro requires both detergent extraction and limited proteolysis. *J Virol* 65:1440-1449.
- Meyer N, Rosenbaum V, Schmidt B, Gilles K, Miranda C, Groth D, Prusiner SB. 1991. Search for a putative scrapie genome in purified prion fractions reveals a paucity of nucleic acids. *J Gen Virol* 72:37-49.
- Morris GA, Freeman R. 1978. Selective excitation in Fourier transform nuclear magnetic resonance. *J Magn Reson* 29:433-462.
- Nguyen JT, Baldwin MA, Cohen FE, Prusiner SB. 1995a. Prion Protein Peptides Induce  $\alpha$ -helix to  $\beta$ -sheet conformational transitions. *Biochemistry* 34:4186-4192.
- Nguyen JT, Inouye H, Baldwin MA, Fletterick RJ, Cohen FE, Prusiner SB, Kirschner DA. 1995b. X-ray diffraction of scrapie prion rods and PrP peptides. *J Mol Biol* 252:412-422.
- Pan KM, Baldwin M, Nguyen J, Gasset M, Serban A, Groth D, Mehlhorn I, Huang Z, Fletterick RJ, Cohen FE, Prusiner SB. 1993. Conversion of  $\alpha$ -helices into  $\beta$ -sheets features in the formation of the scrapie prion proteins. *Proc Natl Acad Sci USA* 90:10962-10966.
- Peerson O, Groesbeek M, Aimoto S, Smith SO. 1995. Analysis of rotational resonance magnetization exchange curves of crystalline peptides. *J Am Chem Soc* 117:7228-7237.
- Pines A, Gibby MG, Waugh JS. 1973. Proton-enhanced NMR of dilute spins in solids. *J Chem Phys* 59:569-590.
- Prusiner SB. 1992. Chemistry and biology of prions. *Biochemistry* 31:12277-12288.
- Prusiner SB, Groth D, Serban A, Koehler R, Foster D, Torchia M, Burton D, Yang SL, DeArmond SJ. 1993. Ablation of the prion protein (PrP) gene in mice prevents scrapie and facilitates production of anti-PrP antibodies. *Proc Natl Acad Sci USA* 90:10608-10612.
- Prusiner SB, McKinley MP, Bowman KA, Bolton DC, Bendheim PE, Groth DF, Glenner GG. 1983. Scrapie prions aggregate to form amyloid-like birefringent rods. *Cell* 35:349-358.
- Raleigh DP, Cruzet F, Das Gupta SK, Levitt MH, Griffin RG. 1989. Measurement of internuclear distances in polycrystalline solids: Rotationally enhanced transfer of spin magnetization. *J Am Chem Soc* 111:4502-4503.
- Raleigh DP, Levitt MH, Griffin RG. 1988. Rotational resonance in solid state NMR. *Chem Phys Lett* 146:71-76.
- Safar J, Roller PP, Gajdusek DC, Gibbs CJJ. 1994. Scrapie amyloid (prion) protein has the conformational characteristics of an aggregated molten globule folding intermediate. *Biochemistry* 33:8375-8383.
- Saito H. 1986. Conformation-dependent  $^{13}\text{C}$  chemical shifts: New means of conformational characterization as obtained by high-resolution solid-state  $^{13}\text{C}$  NMR. *Magn Reson Chem* 24:835-852.
- Schaefer J, Stejskal EO. 1976. Carbon-13 nuclear magnetic resonance of polymers spinning at the magic angle. *J Am Chem Soc* 98:1031-1032.
- Shirley JH. 1965. Solution of the Schrödinger equation with a Hamiltonian periodic in time. *Phys Rev B* 138:979.
- Smith SA, Levante TO, Meier BH, Ernst RR. 1994a. Computer simulations in magnetic resonance—An object-oriented programming approach. *J Magn Reson A* 106:75-105.
- Smith SO, Jonas R, Braiman M, Bormann BJ. 1994b. Structure and orientation of the transmembrane domain of glycoprotein A in lipid bilayers. *Biochemistry* 33:6334-6341.
- Spera S, Bax A. 1991. Empirical correlation between protein backbone conformation and  $\text{C}\alpha$  and  $\text{C}\beta$   $^{13}\text{C}$  nuclear magnetic resonance chemical shifts. *J Am Chem Soc* 113:5490-5492.
- Stahl N, Baldwin MA, Teplow DB, Hood L, Gibson BW, Burlingame AL, Prusiner SB. 1993. Structural analysis of the scrapie prion protein using mass spectrometry and amino acid sequencing. *Biochemistry* 32:1991-2002.
- Stahl N, Borchelt DR, Hsiao K, Prusiner SB. 1987. Scrapie prion protein contains a phosphatidylinositol glycolipid. *Cell* 51:229-240.
- Taraboulos A, Serban D, Prusiner SB. 1990. Scrapie prion proteins accumulate in the cytoplasm of persistently infected cultured cells. *J Cell Biol* 110:2117-2132.
- Thompson LK, McDermott A, Raap J, van der Wielen CM, Lugtenburg J, Herzfeld J, Griffin RG. 1992. NMR study of active site structure in bR: Conformation of schiff base linkage. *Biochemistry* 31:7931-7938.
- Tomita Y, O'Connor EJ, McDermott A. 1994. A method for dihedral angle measurement in solids: Rotational resonance NMR of a transition-state inhibitor of triose phosphate isomerase. *J Am Chem Soc* 116:8766-8771.
- Tycko R, Dabbagh G. 1990. Measurement of nuclear magnetic dipole-dipole couplings in magic angle spinning NMR. *Chem Phys Lett* 173:461-465.
- Vega S. 1992. The Floquet theory of nuclear magnetic resonance spectroscopy of single spins and dipolar coupled spin pairs in rotating solids. *J Chem Phys* 96:2655-2680.
- Wishart DS, Sykes BD. 1994. The  $^{13}\text{C}$  chemical-shift index: A simple method for the identification of protein secondary structure using  $^{13}\text{C}$  chemical shift data. *J Biomol NMR* 4:171-180.
- Zhang H, Kaneko K, Nguyen JT, Livshits TL, Baldwin MA, Cohen FE, James TL, Prusiner SB. 1995. Conformational transitions in peptides containing two putative  $\alpha$ -helices of the prion protein. *J Mol Biol* 250:514-526.